U_3O_8 Addition Effects on Microstructure of UO_2 Pellets Sintered in Reducing Atmosphere

João Antenor[1*], Humberto Riella[1,2]

[1]*Instituto de Pesquisas Energéticas e Nucleares (IPEN / CNEN - SP). Centro do Combustível Nuclear (CECON)*
[2]*Universidade Federal de Santa Catarina*

*[*]**Corresponding Author:** João Antenor, Instituto de Pesquisas Energéticas e Nucleares (IPEN / CNEN - SP). Centro do Combustível Nuclear (CECON), Tel.: +55 11 2819 5623, E-mail.: jpmantenor@usp.br

Abstract

The ability to retain fission products, specifically gases, namely Xenon and Krypton, is a major concern on nuclear fuel development and operation. On PWR's fuels based on uranium dioxyde pellets this is an important matter when operating on high burn up states. It is known that the increase in grain size can increment this capacity. Metal oxides additives can deliver significant results on grain size. However, additives also negatively affect the diffusivity of fission products within the pellet.

Typically, sintered pellets that fail quality control undergo oxidation to generate U_3O_8 powder, which is subsequently incorporated into the composition of green pellets, serving as a pore former. Several investigations aim to enhance the sinterability of U_3O_8 powder in order to promote grain growth during the sintering process without additives. On this work, U_3O_8 powder was produced from non recycled UO_2 powder using two different processes and then added to UO_2 powder to produce pellets. These pellets ware sintered in reducing atmosphere and their grain size was measured by image analysis in order to study the effects of the two different U_3O_8 powder additions to the grain size.

Keywords: UO_2 pellets; Sintering; U_3O_8; Nuclear Fuel

Introduction

Fission gas release is a major concern regarding fuel performance. A fuel with the capacity of retain those gases on its structure can still operate at high burn up levels without increasing the cladding internal pressure compromising safety. One characteristic that most significantly affects the ability to retain fission gas is the pellet microstructure.. Large grain size pellets retain better the fission gases than fine grained ones [1].

Many studies have reported the positive effect of sintering additives on grain size [2, 3, 4]. For instance, [5] obtained grain sizes as large as 70 μm with additives such as Ti and Nb. Although the increase in grain size due to additives has been well established, there is some controversy surrounding this practice. It was verified that UO_2 pellets doped with 0, 5 %wt Nb2O5 had a Xe133 diffusion coefficient ten times higher that that of an undoped pellet at 1500 ºC [6]. In the 1990s, [7] demonstrated through measurements of fractional gas release that the release of fission gases was approximately twice times higher in titania--doped UO_2 pellets compared to undoped pellets with the same grain size. In the 2010s, [8] verified through simulations based on empirical models that this effect was closely related to the availability of Frankel defects created by the cations dissolved in the lattice due to the additives. The same study shows that the creation of vacancies by Frankel defects is responsible not only for enhancements in U4+ diffusivity but also for an increase in the mobility of fission gases.

Since there is this apparent limitation on dopants, many works aiming to improve the grain size using different tools from dopants have been developed. Stoichiometry is an aspect which influences the diffusivity of U cations during sintering temperature range. Many authors have obtained good results regarding the usage of U_3O_8.

U3O8 seeds with controlled particle sizes in UO_2 was used by [9] to obtain grain sizes on the order of 14 μm. In this reference, it is suggested that the larger grain size was promoted by the preferential coalescence of grains originating from U_3O8, which were initially larger.

In the industry, UO_2 pellets which have defects are usually oxidized to U_3O_8 powder and this is added to the UO_2 powder as a recyled material. Recycled U_3O_8 have a low activity [10] and that reflects on the sinterability and grain size of the pellets. some results indicates that it can be one sixth of the UO_2 activity. The recycled U_3O_8 activity could be increased by [11] using cycles of oxidation and reduction.

In [12] it was possible to highly increase the UO_2 pellets grain size adding U_3O_8 and Nb_2O_5. The good results was associated with the increase in U ions mobility due to the additional Nb ions.

This work aims to study the possibility of using U_3O_8 prepared by oxidizing the green UO2 powder instead of the recycled pellets in order to enhance its activity. For this, U_3O8 was prepared via two different processes and then added to UO_2 pellets without any grain size increasing dopant.

Experiments

Sample Preparation

UO_2 powder was obtained from uranium hexafluoride via ammonium uranyl carbonate (AUC) conversion. It was characterized by BET method and by polarometry to verify its O/U ratio.

Additionally, XRD analysis was conducted to confirm the composition of this powder. The Rietveld method was employed for this purpose. This approach utilizes least squares to refine the data while taking into account the theoretical diffraction pattern from the potential phases present in the sample.

This powder was used to produce U_3O_8 considering two routes. In the first route the powder was thermally treated at 400 ºC under air for 1 h, and on the second one, it was treated at 1300 ºC for 1 h under air as well. In this work the U3O8 treated at 400 ºC will be called " U_3O_8 V" and the one produced at 1300 ℃, " U_3O_8 Q". The same characterization processes employed on the UO2 powder was carried out on both U3O8 powders.

The U_3O_8 Q particles has initialized a sinterization process and bonded together due to the high temperature. In order to use it as intended, it was machanically separated with a mortar and pestle kit. Both U3O8 powders ware sieved at a 325 mesh sieve to avoid using agglomerates during the sintering.

Three batches were produced. The first is the reference sample, which contain only UO_2 powder and aluminum diesterate. The second and the third batches was produced by adding one of U_3O_8 powders. The batches was homogenized in a Wab Turbula homogenizer model T2F at 48 rpm by 1 h. Table 1 shows the composition of each batch.

Batch	UO_2 (wt%)	ADS (wt%)	U_3O_8 V (wt%)	U_3O_8 Q (wt%)
A	99,8	0,2	-	-
B	89,8	0,2	10	-
C	89,8	0,2	-	10

Table 1: Batches compositions

The pellets from each batch ware pressed at a pressure ranging from 350 to 400 Mpa and sintered in a Seteram dilatometer model Setsys at 1700 ºC for 4 h, with a temperature increase rate of 5 ºC/min and a cooling rate of 20 ºC/min.

The pellets were longitudinally sectioned and prepared for metallographic analysis through polishing. The polished samples ware thermally etched at 1400ºC for 2h in a CO2 atmosphere.

Microstruture Analysis

The cross´section samples ware observed at a Zeiss optic microscope model Axio at a magnification rate of 50 times. For each sample, 9 pictures ware taken following a 3 x 3 of the sample section prior to the thermal etching. Those micrographs ware used in the porosity analysis. After the thermal etching, 25 pictures ware taken covering all the section, considering a 5×5 matrix. The pictures ware processed and analyzed in the software Quantikov [13, 14]. The pictures ware segmented in order to automatize the grain size and pore measurement, which ware made by the equivalent diameter.

Data from the equivalent diameters ware analyzed employing the software capability to calculate the Saltykov classes, which considers a three dimensional distribution of the grains approximated as spheres.

Results

Figure 1 shows the diffractograms of the three powders used in this work. The peaks of the U3O8 powders match the PDF 65-6461 (CIF 16559) and the Rietveld analysis confirmed the composition on 100% of this phase, ensuring that the method used to produce the U3O8 powders was effective. The diffractogram of the UO_2 powder shows small peaks corresponding to U3O8, which were identified according to PDF 65-6461. The peaks of UO_2 match the expected pattern according to PDF 74-2432 (CIF 246851). The intensity of the U_3O_8 phase peaks is lower than that of the UO_2 peaks, as expected. The quantification of phases using the Rietveld method indicated a composition of 4.95% U_3O_8 in the sample
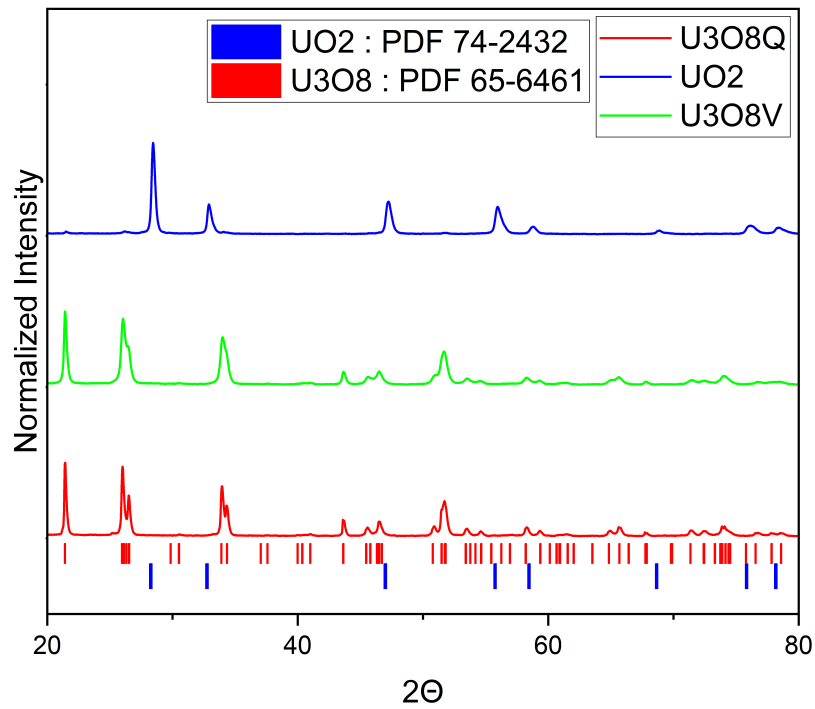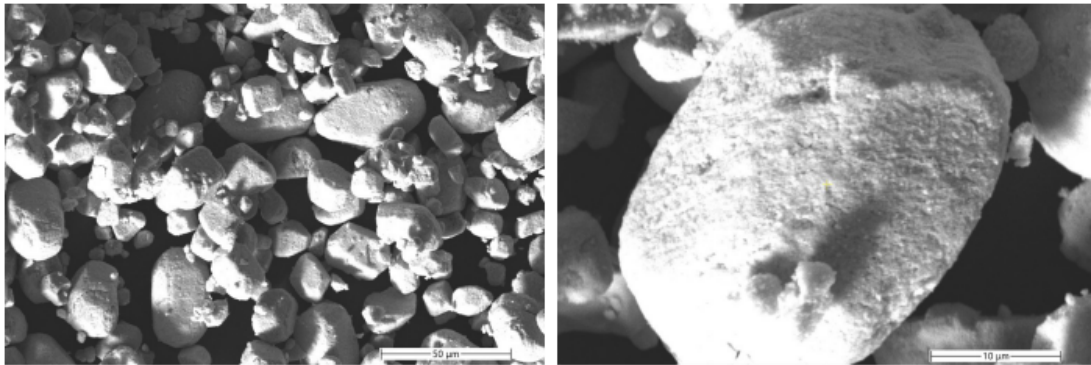
Figure 1: Diffractogram for phase identification. UO$_2$ powder

Figure 2 presents the microstructural aspects of the powders. The it can be observed that the morphology of the UO2 powder is comparable to that of other studies using the same material [15]. It has the typical morfology of UO2 obtained by the AUC wet route.
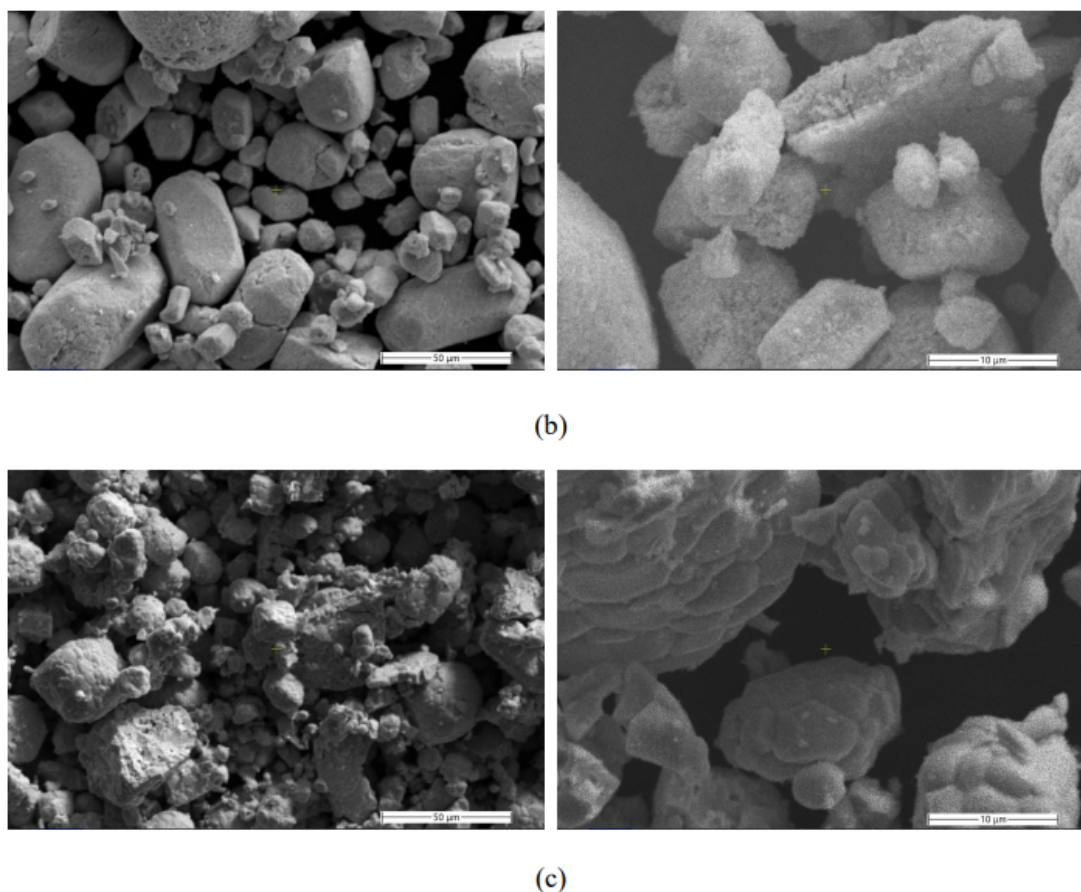

(a)

Figure 2: SEM micrographs. (a) UO_2 powder, (b) U_3O_8 V powder and (c) U_3O_8 Q powder

The surface aspect of both U_3O_8 powders reflects the processing conditions. The powder processed at 1300°C, due to the high temperature, underwent sintering and formed agglomerates, which required mechanical comminution to separate the aggregates as observed earlier. It is possible to observe fractured particles as a result of the comminution process. The surface aspect of the U_3O_8 processed at 400°C shows significant similarity to the UO_2 powder.

Table 2 presents the area densities measured by BET method for each material.

Powder	Area density (m^2/g)	Standard deviation (m^2/g)
UO_2	4,46	0,15
U_3O_8 V	4,61	0,13
U_3O_8 Q	0,08	0,01

Table 2: Powders area densities

Table 3 presents the density of the pellets of each composition as a percentage of the theoretic density 10,95 g/cm^3 before (green pellets) and after sintering.

Condition	Green density (% TD)	Sintered density (%TD)
A (O/U 2.26)	50.55%	95.04%
B (10%U_3O_8 V)	51.68%	94.40%
C (10%U_3O_8 Q)	54.04%	92.13%

Table 3: Green and sintered density for each condition

Figure 3 presents the shrinkage and shrinkage rate of the U_3O_8 additivated samples compared to the Pure UO2 sample.
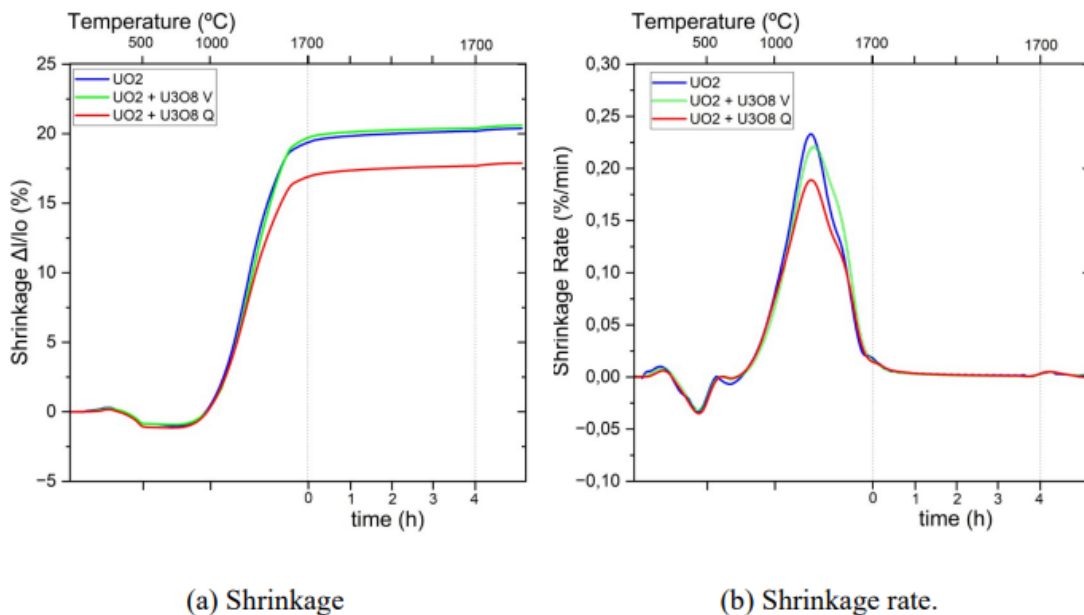

(a) Shrinkage   (b) Shrinkage rate.

Figure 3: Sintering curves

The condition with the worst performance regarding sintering was the one with U_3O_8 Q. It showed the least shrinkage and the smallest shrinkage rate.Figure 4 illustrates the overall aspect of the porosity in the sintered pellets.
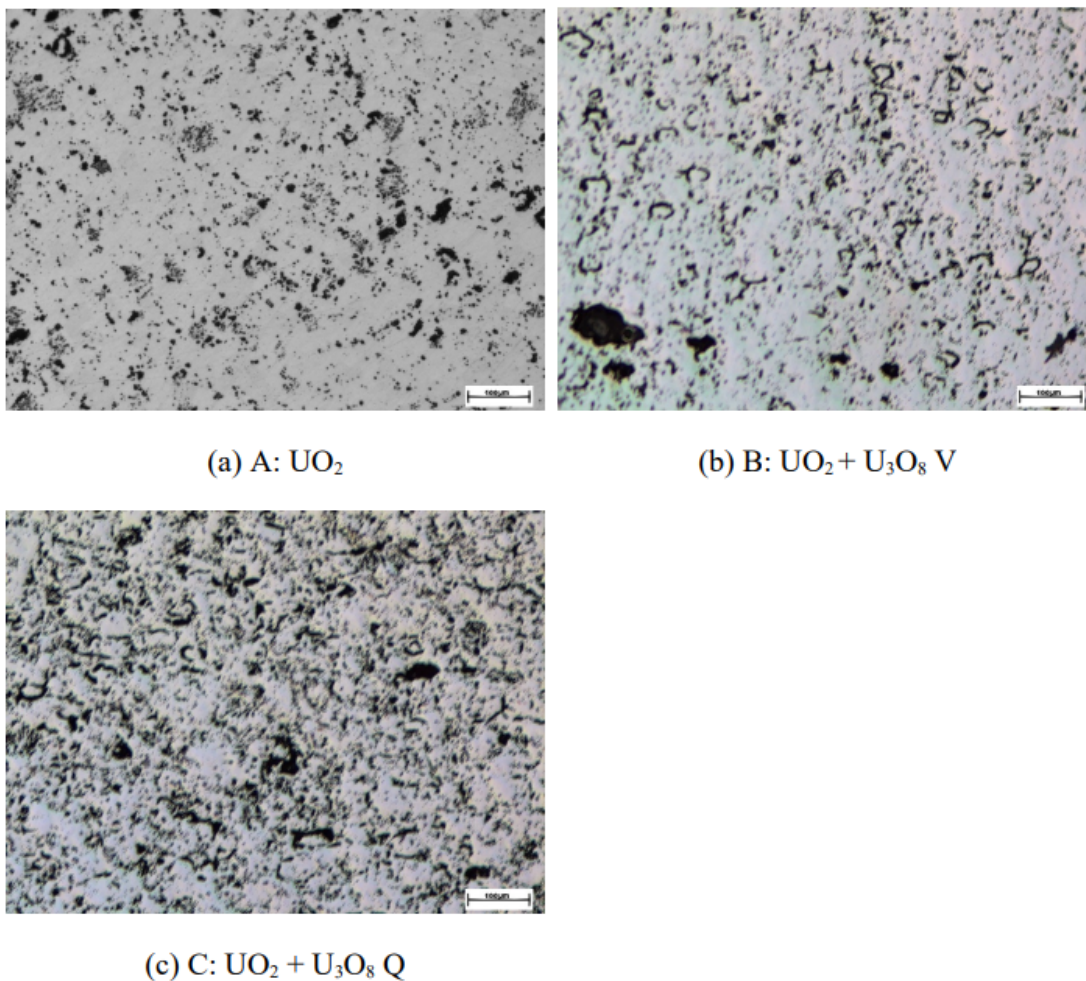

(a) A: UO_2

(b) B: $UO_2 + U_3O_8$ V

(c) C: $UO_2 + U_3O_8$ Q

Figure 4: Micrographs illustrating the typical pores morphological aspect of the sintered pellets

The micrographs suggest that the pellet with U_3O_8 Q has higher porosity and had less densification.Table 4 shows the pore measurement data.

Composition	Medium diameter (µm)	Minimum diameter (µm)	Maximum diameter (µm)	Standard Deviation (µm)
A: UO_2	5.9	1.0	71.3	4.8
B: UO_2+ 10% U_3O_8 V	4.3	1.0	87.0	4.6
C: UO_2 + 10% U_3O_8 Q	4.1	1.0	79.0	5.6

Table 4: Pore measures per composition

The data regarding grain size measurement are presented in Table 5. Figure 5 illustrates micrographs of grain boundaries from the 3 conditions.

Composition	Medium diameter (µm)	Minimum diameter (µm)	Maximum diameter (µm)	Standard Deviation (µm)
A: UO_2	12,4	0,3	66,6	8,1
B: UO_2+ 10% U_3O_8 V	7,1	0,5	30,9	4,3
C: UO_2 + 10% U_3O_8 Q	7,2	0,3	34,0	4,6

Table 5: Grain size measures per composition

(a) A: UO_2

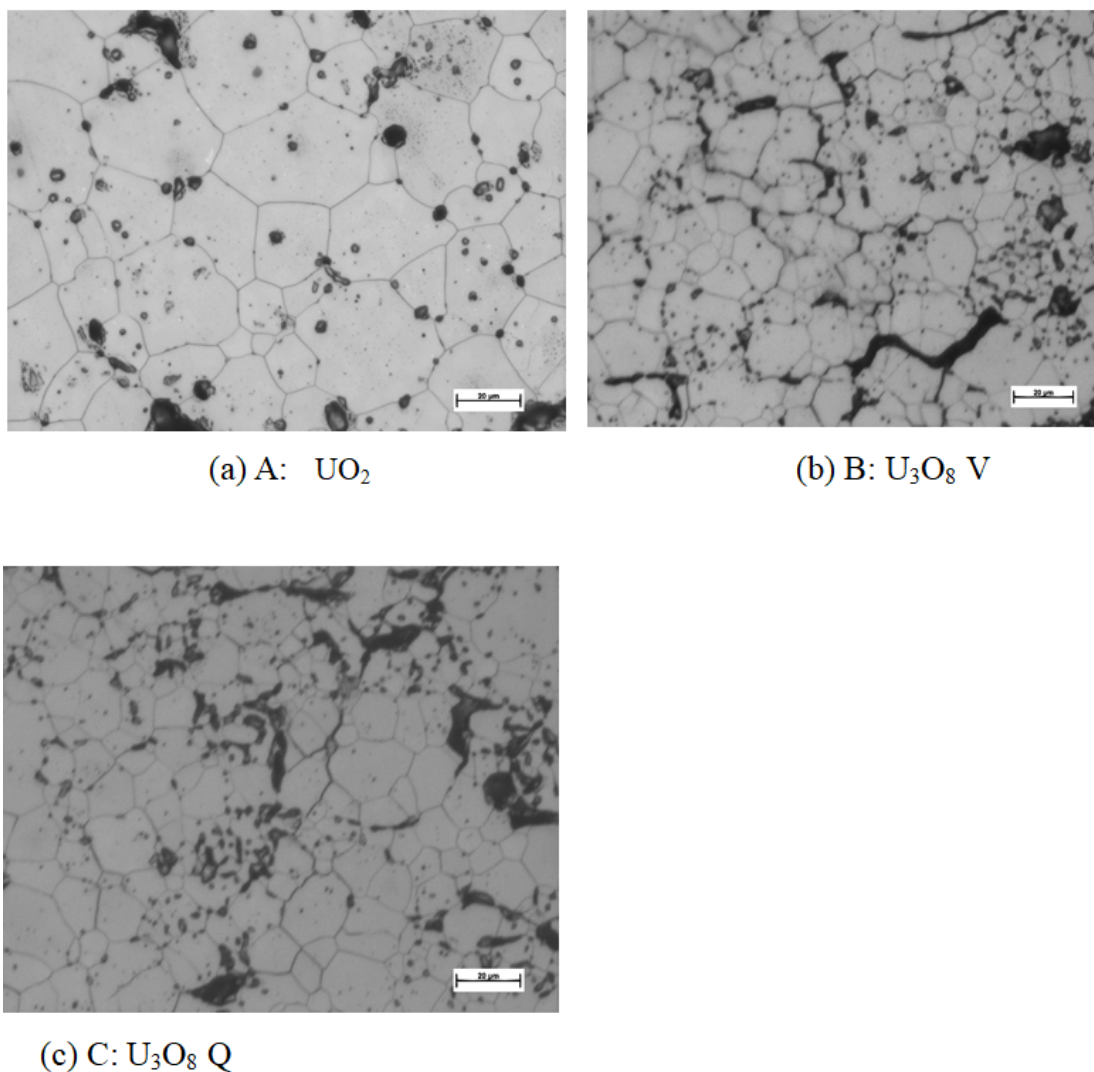(b) B: U_3O_8 V

(c) C: U_3O_8 Q

Figure 5: Micrographs of the samples microstructures

Figure 6 presents the Saltykov grain size distribution curves. It permits the visualization of the similarity between the grain size obtained for the pellets additivated with the two types of U_3O_8 studied. It is also evident how distinct the pellet with no additives is from the behavior of the others. The difference is characterized by the attainment of larger grain sizes with higher frequency and the relatively lower quantity of smaller-sized grains.
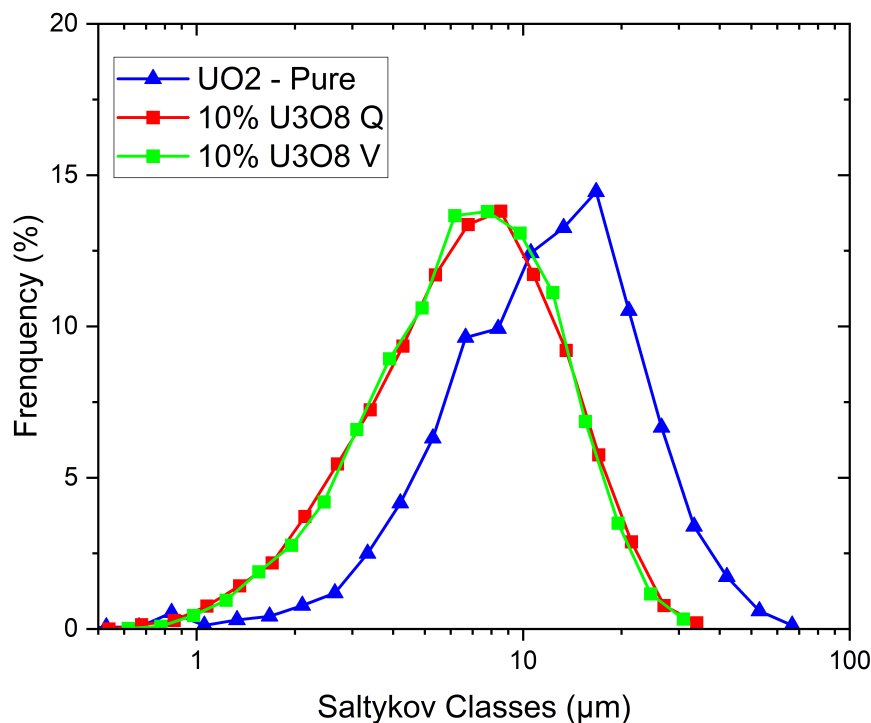

Figure 6: Saltykov classes frequency for the different compositions

Discussion

On the pure UO_2 pellets was identified the presence of U_3O_8 which is evidenced by the peaks between 20 and 27º. Furthermore, the morphology of the peaks indicates some important aspects about the arrangement of the U_3O_8 phase in the material. As observed in Figure 7, the diffraction peak corresponding to the 100 plane of U3O8 exhibits asymmetry, as well as being slightly broadened and shifted to the right, i.e., at a higher 2Θ value. The shift towards a higher diffraction angle indicates the presence of compressive microstrains in the lattice [16]. This strain is believed to originate from the formation of U_3O_8 within the UO2 matrix. It is understood that the strain arises from the difference between the crystal structures, which represents different volume and density, as U_3O_8 is orthorhombic while UO_2 has a fluorite-type structure. Additionally, due to the transformation occurring at low temperatures, the diffusion kinetics are reduced, making it difficult for the two phases to segregate.
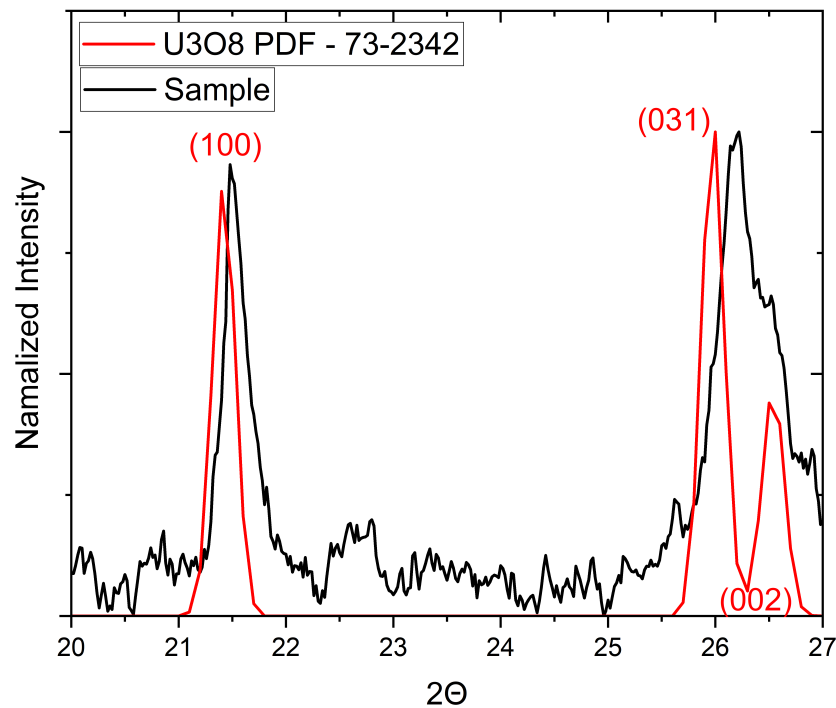
Figure 7: U_3O_8 peaks on UO_2 powder comparison analysis with PDF – 73-2342

SEM micrographs showed similarity between the superficial aspects of UO_2 powder and the U3O8 V. This similarity is reflected in the surface area density measured by BET. The transformation to U_3O_8 V slightly increased the area density of the original powder but they still maintain the compatibility of the values, on the other hand, the U_3O_8 Q had a significant decrease in this characteristic. It is expected that the area was diminished due to the initial sintering that this material suffered as observed in the SEM micrographs on Figure 3.

The sample with U_3O_8 Q had the lowest level of densification, as evidenced by the lower hydrostatic density among the studied conditions. Considering the lower limit of 95% DT, the samples which had U_3O_8 additions of any kind did not meet this requirement.

The density behavior can be verified on the sintering curves as well. U3O8 Q had a negative influence on sinterability, as the shrinkage level was lower than that of the non-additivated sample. Additionally, the additivated pellet in this condition had a lower maximum shrinkage rate, as observed in Figure 5 (b). This negative effect reflects the small area density observed in table 5 for this material.

The green U_3O_8 did not significantly affect the shrinkage or shrinkage rate during sinterig. This behavior can be related to the compatibility of area density observed for both components of the Batch.

These observations indicate better sinterability of the green U_3O_8 compared to the burnt U_3O_8.

A phenomenon related to the temperature range below the start of the sintering is the change in the oxidation state of uranium ions due to excess of oxygen. This leads to tetravalent uranium ions to become hexavalent, which reduces the ionic radius and consequently the lattice parameters of the unit cell. On a macro scale, this would represent a volume reduction. By removing the excess oxygen due to the reducing atmosphere, the lattice parameter returns to the stoichiometric condition, i.e., an O/U ratio of 2.0, leading to an expansion of the volume.

Another phenomenon associated with this temperature range, up to 800°C, is the reduction of the U_3O_8 phase to UO_2. As discussed earlier, this transformation is associated with the creation of pores.

Consistent with the dilatometry and hydrostatic density results, visually, it is evident by the micrographs on Figure 4 that the sample additivated with burnt U_3O_8 has a higher porosity then the others.

Observing the results on table 4, all pellets are considered suitable regardless of the pellet composition, considering that all the medium pore size is close to 5 μm and there are no pore bigger than 500 μm. Nevertheless, the overall behavior of the pores are very similar.

The average grain size obtained for the pure UO_2 sample was negatively affected by the addition of U_3O_8, regardless of the type of U_3O_8. The average grain size was reduced from 12.4 μm to approximately 7 μm in both cases.

The significant reduction in grain size observed by the addition of U_3O_8, in both conditions, may be related to the generation of pores promoted by this phase during its reduction. It is proposed here that due to the concentration of this phase in the added powder particles, porosity would be more intensely formed in these particles, creating regions of higher pore concentration, which is referred to in the literature as pore clusters [8]. These clusters of pores would hinder diffusive processes between grains in their proximity, resulting in smaller grains due to the lack of coalescence in these regions. Figure 8 illustrates a region where smaller grains are concentrated within a cluster of pores. It is also possible to observe in the same figure that regions with fewer pores exhibit larger grain sizes.
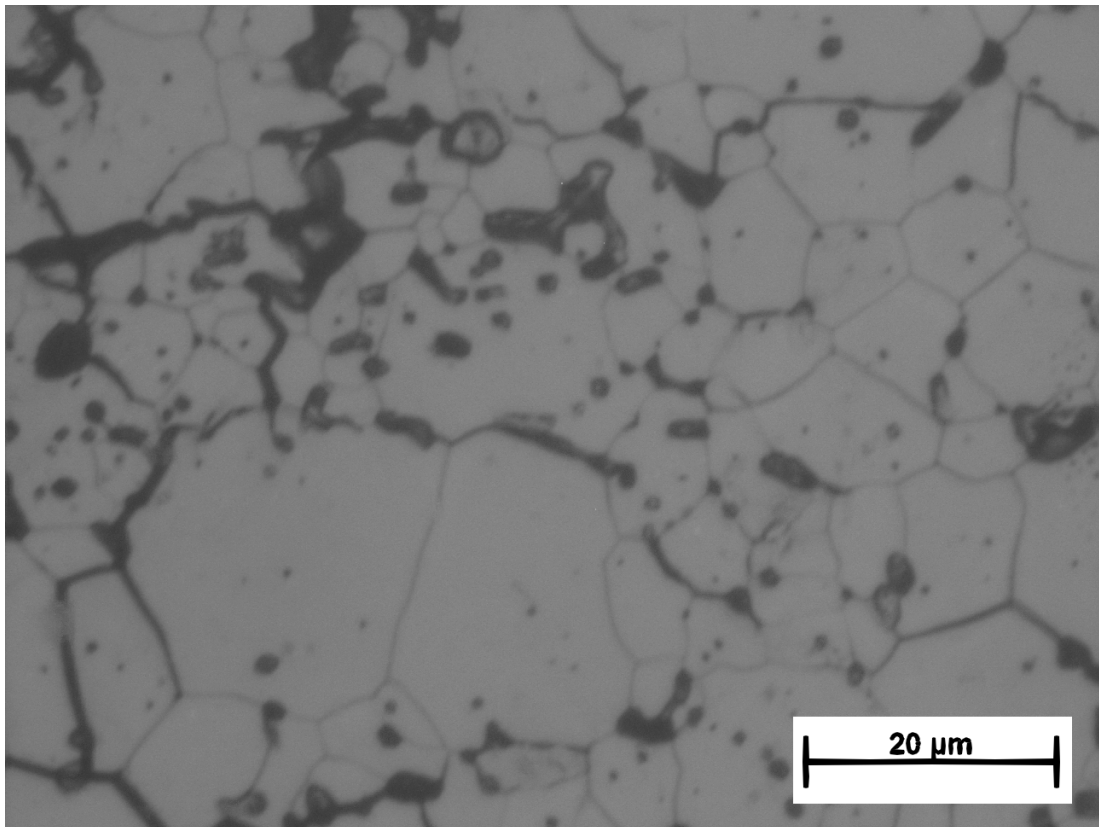

Figure 8: Example of the pore cluster influence on grain size development. Picture taken from the sample with U3O8 Q

It is important to highlight the growth observed in the pure UO_2 and the possibility of its relationship with the U_3O_8 identified in the X-ray analysis of the powder. In this material, it is understood that U_3O_8 is located on the surface of the UO_2 powder as a result of ambient temperature oxidation. This disposition suggests that the growth mechanism would involve the uniform generation of pores around the UO_2 particles during the reduction of U_3O_8. This uniform distribution of pores during sintering would promote mass transport through the process of evaporation-condensation.

The higher grain size observed on the pellet sintered from the UO_2 powder with no U_3O_8 addition showed the higest grain size among the conditions studied in this work. As observed by Rietveld analysis, this powder already had some U_3O_8, which is believed to be disposed at the surface of the particles. This result indicates that this condition can display a better performance considering the fission gas retention within the pellet.

Conclusion

Based on the results obtained and the discussions presented, it can be concluded that:

1. The sinterability of U_3O_8 powder and its effects on the sinterability of the mixture are closely related to the surface area density, which is influenced by the oxidation method employed to produce the U_3O_8 powder.

2. Considering the method of adding U_3O_8 used in this work, which involved mixing the pass-through powder on a 325 mesh sieve with the UO_2 powder in a 10% ratio, it was not possible to achieve grain size increments. This observation applies to both green and burnt U_3O_8. The localized porosity generated by the reduction of U_3O_8 during sintering acted as anchor points for grain boundaries, limiting grain growth and reducing the average grain size.

3. The sintering of UO_2 with an O/U ratio of 2.26, possibly due to the homogeneous distribution of U_3O_8 in its structure and the hyperstoichiometry, resulted in a grain size larger than the minimum acceptable in industrial pure UO_2 pellets without the use of sintering additives.

References

1. HIRAI M et al. (2000) Grain size effects on fission gas release and bubble swelling at high burnup. International topical meeting on light water reactor performance.

2. STEHLE H, ASSMANN H, MAIER G (1983) Review of UO_2, Powder and Pellet Fabrication Under the Aspects of In-Reactor Fuel Behavior. In: IAEA/CNEA International Seminar on Heavy Water Reactor Fuel Technology.

3. HARADA Y (1996) Sintering behaviour of niobia-doped large grain UO2 pellet. Journal of nuclear materials, 238: 237-243.

4. DOOIES BJ (2008) Enhancement of uranium dioxide thermal and mechanical properties by oxide dopants ((Doctoral dissertation). University of Florida.

5. RADFORD KC, POPE JM (1983) UO_2 fuel pellet microstructure modification through impurity additions. Journal of nuclear materials 116: 305-13.

6. UNE K, TANABE I, OGUMA M (1987) Effects of additives and the oxygen potential on the fission gas diffusion in UO2 fuel. Journal of nuclear materials 150: 93-9.

7. YUDA R et al. (1997) Effects of pellet microstructure on irradiation behavior of UO_2 fuel. Journal of nuclear materials 248: 262-7.

8. COOPER MWD, STANEK CR, ANDERSSON DA (2018) The role of dopant charge state on defect chemistry and grain growth of doped UO_2. Acta Materialia 150: 403-13.

9. SONG KW et al. (2003) Grain size control of UO_2 pellets by adding heat-treated U_3O_8 particles to UO_2 powder. Journal of Nuclear materials 317: 204-11.

10. Costa DR, Ezequiel F J, Carnaval JPR, Barbosa RA (2014) Effects of U_3O_8 Addition on Microstructure of UO_2-Doped and Undoped Ceramic Fuel Pellets, 21º CBECIMAT - Congresso Brasileiro de Engenharia e Ciência dos Materiais.

11. HOYT RC et al. (1979) AIROX dry reprocessing of uranium oxide fuels. Report ESG-DOE-13276

12. SONG KW, KIM KS, KANG KW, JUNG YH (2000) "Sintering of Mixed UO_2 and U_3O_8 Powder Compacts", J. Nuclear Materials 277: 123 -9.

13. Quantikov Image Analyzer. https://quantikov.webnode.page/ visited on 06/07/2023

14. PINTO L (1996) Quantikov um analisador microestrutural para o ambiente windows sup (TM).

15. DE FREITAS AC et al. (2022) Effects of aluminum distearate addition on UO_2 sintering and microstructure. Progress in Nuclear Energy 153: 104440.

16. CULLITY BD, STOCK SR (2014). Elements of X-ray diffraction 3rd ed. 2014. Pearson, Edinburgh Gate, Harlow, Essex, England.